ARTICLES

Deactivation Rate Constants of OH($X^2\Pi_i$, $v = 1-4$) by Collisions of NH_3

Katsuyoshi Yamasaki,* Akihiro Watanabe,† Teruaki Kakuda, and Ikuo Tokue

Department of Chemistry, Niigata University, Ikarashi, Niigata 950-2181 Japan

Received: January 12, 2000; In Final Form: July 19, 2000

Collisional deactivation of OH($X^2\Pi$, v=1−4) by NH_3 has been studied using pulsed laser photolysis coupled with the pulsed laser probe technique. Mixtures of $O_3/NH_3/N_2$ were photolyzed at 248 nm, and time-resolved OH populations were monitored via the $\Delta v = 0$ and −3 sequences of the $A^2\Sigma^+-X^2\Pi_i$ transition. The following deactivation rate constants at 298 ± 1 K were obtained: $(2.9 \pm 0.2) \times 10^{-11}$ for $v = 1$, $(1.1 \pm 0.2) \times 10^{-10}$ for $v = 2$, $(3.4 \pm 0.4) \times 10^{-10}$ for $v = 3$, and $(4.1 \pm 0.3) \times 10^{-10}$ for $v = 4$ in units of cm^3 $molecule^{-1}$ s^{-1} (the errors are 2σ). The present study is the first report on the rate constant for OH(v=4) + NH_3 reaction. The deactivation of OH($v \leq 3$) by NH_3 can be elucidated by nonresonant V−V energy transfer caused by long-range interaction; that of $v = 4$ deviates from the gap law.

1. Introduction

The hydroxyl radical OH($X^2\Pi_i$) has been the object of a great deal of research because of its importance in the chemistry of the atmosphere and combustion. Vibrationally excited OH is produced atmospherically by the following reactions: $H + O_3 \rightarrow OH(v \leq 9) + O_2$ in the mesopause (85 km altitude), and $O(^1D) + H_2O \rightarrow 2OH(v \leq 3)$ in the stratosphere.[1] The reaction of OH with NH_3 produces amidogen (NH_2) which removes NO_x via a process called thermal deNO_x: $NH_2 + NO \rightarrow H_2O + N_2$.[2,3] The rate constants of the OH + NH_3 reaction have been measured over a wide range of temperatures, and the resulting recommended value is $(1.7 \times 10^{-12}) \exp[-710 \pm 200\ K/T]$ cm^3 $molecule^{-1}$ s^{-1}, and the rate constant at 298 K is 1.6×10^{-13} cm^3 $molecule^{-1}$ s^{-1}.[4]

There have been many studies on deactivation of vibrationally excited OH($X^2\Pi_i$) by various collision partners.[5−24] Laser-induced fluorescence (LIF) excited with a tunable laser is widely used to detect OH. Low vibrational levels ($v = 0-2$) have been monitored by LIF via the $\Delta v = 0$ or −1 sequences of the $A^2\Sigma^+-X^2\Pi_i$ system, and high vibrational levels with $v = 7$,[21] 8,[23,25] 9,[25] 10,[23] 11,[23] and 12[18] have been detected via the vibrational bands of the $B^2\Sigma^+-X^2\Pi_i$ transition.

Relatively fewer measurements have been reported for the middle range of vibrational levels, $3 \leq v \leq 6$. Teitelbaum et al.[14] have employed time-resolved Fourier transform infrared spectroscopy (FTIR) to measure the rate constants for OH(v=1−4) + O_3, and Dodd et al.[19] have determined relaxation rate constants for OH(v=1−6) + O_2 and OH(v=1−4) + CO_2 using the same technique. Wiesenfeld's group[26,27] has reported that the LIF via $\Delta v = -2$ and −3 sequences are feasible for the detection of $v = 3$ and 4, and they have studied the product vibrational distributions of the reactions between $O(^1D)$ and hydrides. We have applied the detection of OH via $\Delta v = -3$ sequence to a kinetic study, and reported deactivation rate constants for OH(v=1−4) + CH_4.[24] Silvente et al.[22] have given the overall rate constants of OH(v=1−3) + H_2O and + CH_4 using the LIF via $\Delta v = -1$ sequence. They measured the rate constants for OH(v=1,2) + NH_3 using $\Delta v = -1$ sequence, although they did not measure those for $v \geq 3$.

In the present study, we have produced vibrationally excited OH in a chemical process, $O(^1D) + NH_3 \rightarrow OH(v \leq 4) + NH_2$, with a pulsed laser, and recorded the time-resolved populations of OH($^2\Pi_i$) on $v = 0-4$ levels using the $\Delta v = 0$ sequences (v = 0, 1, and 2) and $\Delta v = -3$ sequences (v = 3 and 4) of the $A^2\Sigma^+-X^2\Pi_i$ system. The temporal profiles of $v = 1$, 2, and 4 were analyzed by single-exponential least-squares fits. For v = 3, because the production and consumption rates are relatively close, both double-exponential fits and a linear integration analysis were used to obtain the deactivation rate constants.

2. Experimental Section

Because the experimental apparatus used in the present study has been described previously,[24,28] only the significant features of the present study are described here. A flow of the mixture of O_3 and NH_3 in a N_2 carrier gas was irradiated with a 248 nm beam from a KrF laser (Lambda Physik LEXtra50, 2 mJ cm^{-2} incident at the flow cell). The reaction $O(^1D) + NH_3 \rightarrow OH + NH_2$ ($\Delta H°_{298} = -165$ kJ mol^{-1}) was used to prepare vibrationally excited OH($v \leq 4$). The N_2 buffer was effective in limiting the production of OH to very short times, because N_2 is an efficient quencher of $O(^1D)$ to $O(^3P)$: $k = 2.6 \times 10^{-11}$ cm^3 $molecule^{-1}$ s^{-1},[4] and because the reaction of $O(^3P)$ with NH_3, k(298 K) $= 7 \times 10^{-17}$ cm^3 $molecule^{-1}$ s^{-1},[29] is much slower than that of $O(^1D) + NH_3$: 2.5×10^{-10} cm^3 $molecule^{-1}$ s^{-1}.[4]

Vibrational levels of OH($X^2\Pi_i$, v=0−4) were detected by laser-induced fluorescence (LIF) via the $A^2\Sigma^+-X^2\Pi_i$ transition using a frequency-doubled dye laser (Lambda Physik LPD-3002

* Author to whom correspondence should be addressed. Fax: +81 25 262 7530. E-mail: yam@scux.sc.niigata-u.ac.jp.

† Department of Applied Chemistry, Kobe City College of Technology, Gakuen-Higashi-machi, Nishi-ku, Kobe 651-2194, Japan.

10.1021/jp000172i CCC: $19.00
Published on Web 09/15/2000

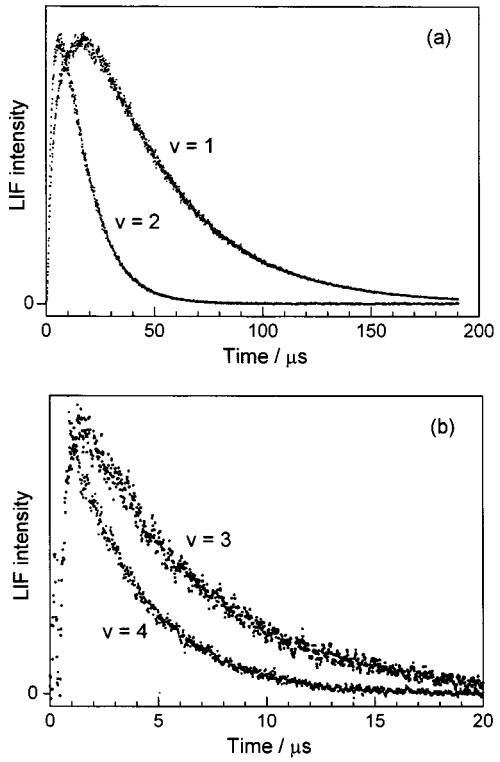

Figure 1. Time-dependent profiles of laser-induced fluorescence signals from OH($X^2\Pi_i$): (a) $v = 1$ and 2, and (b) $v = 3$ and 4. Scanned step sizes of the delay were 100 μs, (a); 18 ns, (b). $P_{O_3} = 0.5$ mTorr and $P_{NH_3} = 20$ mTorr. All the profiles are normalized to their maximum intensities. It should be noted that the scales of abscissa of (a) and (b) are different by a factor of 10.

with a BBO III crystal, 100−700 μJ cm^{-1} incident at the cell) pumped with a Nd^{3+}:YAG laser (Spectron SL803). The LIF of 0−0, 1−1, 2−2, 3−3, 0−3, and 1−4 bands were observed. Because the fluorescence yields of OH($A^2\Sigma^+$, $v' \geq 3$) are very low because of efficient predissociation,[30,31] a sequence with $\Delta v = -3$ instead of $\Delta v = 0$ was excited to detect $v'' = 3$ and 4. The rotational lines excited were $P_1(2)$ of the 0−0 (308.6 nm), 1−1 (314.3 nm), and 2−2 (320.8 nm) bands, and $Q_1(2)$ of the 0−3 (449.2 nm) and 1−4 (451.0 nm) bands, respectively. The $Q_1(2)$ lines blend a little with the $^qP_{21}(2)$ satellite lines; however, no problems occurred because the lines originate in the same lower rotational level.

The photolysis and probe lasers were counterpropagated and overlapped in the flow cell, and the LIF was collected with a lens (f = 80 mm) and detected with a photomultiplier tube (PMT) (Hamamatsu R928) mounted perpendicularly to the laser beams. The signal from the PMT was averaged with a gated integrator (Stanford Research SR250) and stored on a computer. Rate constants for the rotational relaxation of OH($X^2\Pi_i$, v=0, N=1−14) by N_2 have recently been reported to be 2.6×10^{-11} cm^3 molecule^{-1} s^{-1},[32] giving a relaxation time of about 250 ns by N_2 at 5 Torr. The intensity of LIF due to a single rotational line after the time for exhaustion of O(^{1}D) is proportional to the population of each vibrational level. Temporal profiles of vibrational levels of interest were observed by scanning the delay time between the photolysis and the probed laser, with a step size of 7−100 ns. The typical number of data points in a profile was 2000. At least three profiles were recorded for a single vibrational level, and averaged data were analyzed.

The flow rates of all the sample gases were controlled with calibrated mass flow controllers (Tylan FC-260KZ and STEC SEC-400 mark3), and several linear flow velocities within 1−10 m·s^{-1} were used. Total pressure in the flow cell (1−10 Torr) was monitored with a capacitance manometer (Baratron 122A, 10 Torr full scale). The total pressure measurement together with the mole fractions as measured by the flow controllers gave the partial pressures of the reagents. Ozone was prepared by electric discharge in pure oxygen (Toyo-Sanso, 99.9995%) with a homemade synthesizer and stored in a 3 dm^3 glass bulb with N_2 (1% dilution). The partial pressure of O_3 was fixed at 0.5 mTorr. Highly pure grade N_2 (Nihon-Sanso, 99.9999%) and NH_3 (Nihon-Sanso, 99.999%) were used without further purification.

3. Results and Discussion

Figure 1 shows the time-dependent profiles of the four vibrational levels ($v = 1-4$) of OH($X^2\Pi_i$) observed at 20 mTorr of NH_3. The initially prepared OH($v \leq 4$) undergo the following reactions:

$$\mathrm{OH}(v) + \mathrm{OH}(v') \rightarrow \mathrm{OH}(v+1) + \mathrm{OH}(v'-1) \quad (1)$$

$$\mathrm{OH}(v) + \mathrm{O_3} \rightarrow \mathrm{OH}(v-1) + \mathrm{O_3} \quad (2a)$$

$$\rightarrow \text{products} \quad (2b)$$

$$\mathrm{OH}(v) + \mathrm{N_2} \rightarrow \mathrm{OH}(v-1) + \mathrm{N_2} \quad (3)$$

$$\mathrm{OH}(v) + \mathrm{NH_3} \rightarrow \mathrm{OH}(v-1) + \mathrm{NH_3} \quad (4a)$$

$$\rightarrow \text{products} \quad (4b)$$

$$\mathrm{OH}(v) \rightarrow \mathrm{OH}(v') + h\nu \quad (5)$$

$$\mathrm{OH}(v) \rightarrow \text{diffusion} \quad (6)$$

The concentration of O(^{1}D) produced in the O_3/248 nm photolysis is estimated to be about 5.5×10^{11} atoms cm^{-3} from the photoabsorption cross section of O_3 at 248 nm, 1.08×10^{-17} cm^2;[4] the O(^{1}D) yield, 0.9;[4] the photolysis laser fluence, 2 mJ cm^{-2}; the beam diameter of the photolysis laser, 5 mm; and the concentration of O_3, 0.5 mTorr. A large portion (93%) of the O(^{1}D) is quenched by N_2 of 5 Torr; the remaining 7% reacts with NH_3, producing OH of about 4×10^{10} molecules cm^{-3} at the typical NH_3 pressure (40 mTorr). It takes about 1.1 μs for 99% of the initially prepared O(^{1}D) to be consumed in quenching or reactions.

Teitelbaum et al.[14] have reported that the rate constants for v = 3 and 4 of (1) are near the gas-kinetic rate, and those of (2) are smaller than 1.4×10^{-11} cm^3 molecule^{-1} s^{-1}. Time constants of the reactions are estimated to be about 125 ms for (1) and 4.4 ms for (2) under the present experimental conditions. Although there has been no report on the rate constants of (3) for higher vibrational levels than v = 2, the previous reports show a vibrational level dependence: $<10^{-14}$ for v = 2,[15,17] $<6 \times 10^{-13}$ for v = 7,[21] $<5 \times 10^{-13}$ for v = 9,[20] $(7 \pm 4) \times 10^{-13}$ for v = 8,[23] and $(1.6 \pm 0.6) \times 10^{-12}$ for v = 10,[23] in units of cm^3 molecule^{-1} s^{-1}. It can, therefore, be assumed that the rate constants of (3) even for $v \geq 3$ are at most 10^{-13} cm^3 molecule^{-1} s^{-1}, and consequently, the relaxation by N_2 (3) with long time constant can be negligible in comparison with (4) of interest.

Radiative decay processes (5) are known as the Meinel system and an origin of atmospheric nightglow.[33,34] Langhoff et al.[35] have reported that the radiative lifetimes of vibrational levels v = 1−15 decrease with vibrational quantum number v: the lifetimes of v = 1, 2, 3, and 4 are 92.9, 45.0, 28.0, and 19.4 ms, respectively. These are much longer than the time scale of the actual observation in the present study.

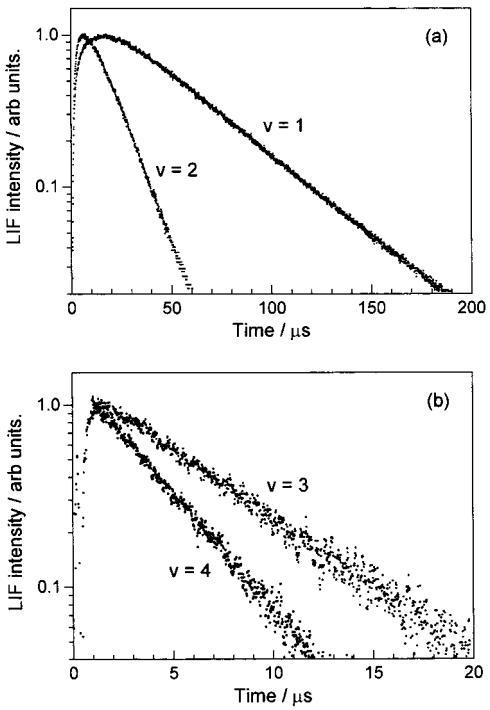

Figure 2. Semilogarithmic plots of time-dependent profiles of LIF signals. The data are the same as those in Figure 1. OH(v=1,2) show single-exponential decay after 50 and 25 μs; OH(v=4) shows an entire straight line; OH(v=3) shows a slight positive curvature, indicating that the rates of relaxation to and from $v = 3$ are close each other.

Reverse processes of (4a) are estimated by the principle of detailed balancing. The rates for backward reactions of (4a) are smaller than those of forward ones by a factor of $\exp[-(E_v - E_{v-1})/k_BT]$, where E_v is an energy of vibrational level v and k_B is the Boltzmann constant. Vibrational energy spacings E_4-E_3, E_3-E_2, E_2-E_1, and E_1-E_0 are 3078, 3240, 3404, and 3570 cm^{-1}, and thus 3.5×10^{-7}, 1.6×10^{-7}, 6.9×10^{-8}, and 3.3×10^{-8} are the ratios of backward to forward, respectively. As a result, the backward reactions of (4a) can be considered negligible in the analysis.

As described above, reactions 1, 2, 3, and 5 are negligibly slow under the present experimental conditions. Because the pseudo-first-order conditions [OH] ≪ [NH_3], [N_2] are satisfied in the present study, rate equations for v (except $v = 4$) are expressed by the following:

$$\frac{d[OH(v)]}{dt} = k_{v+1,v}[NH_3][OH(v+1)] - \{(k_{v,v-1} + k_v)[NH_3] + k_d\}[OH(v)] \quad (7)$$

where $k_{v,v-1}$ corresponds to the rate constants for the vibrational relaxation from the level v to $v - 1$ by NH_3 (4a), k_v is a reactive removal rate constant for the level v (4b), and k_d is the first-order rate constant for the diffusion loss (6). Because all the vibrational levels have the same mass, it is assumed that the rates of diffusion are the same. The sum $k_{v,v-1} + k_v$ is defined to be a total removal rate constant k_v^{tot} of the level v. Because the highest populated vibrational level is $v = 4$, from the heat of reaction, $O(^1D) + NH_3 \rightarrow OH + NH_2$: $\Delta H°_{298} = -165$ kJ mol^{-1}, there are no terms of OH($v \geq 5$) in eq 7. Because $v = 4$ undergoes only decay, the profiles can be readily fit to a single-exponential form, and actually the semilogarithmic plots of observed profiles are linear, as shown in Figure 2b. The time dependences of $v \leq 3$, on the other hand, are given by the following linear combination of exponential terms:[36,37]

$$[OH(v)] = \sum_{i=v}^{4} C_i \exp[-(k_i^{tot}[NH_3] + k_d)t] \quad (8)$$

where C_i are time-independent constants and given by the complicated expressions composed of the initial populations and rate constants related to the level i and higher levels. If the first-order decay rate of the level v of interest k_v^{decay} ($\equiv k_v^{tot}[NH_3\} + k_d$) is sufficiently slower than those of higher levels, the profiles of [OH(v)] at large t is represented by a single term: $C_v \exp(-k_v^{decay}t)$. As seen in Figure 2a, $v = 1$ and $v = 2$ show clear single-exponential decay after 50 and 25 μs, respectively. Therefore, total removal rate constants k_i^{tot} for $v = 1$, 2, and 4 have been obtained from semilogarithmic analyses of time-dependent profiles recorded at various NH_3 pressures: $(2.9 \pm 0.2) \times 10^{-11}$ for v=1, $(1.1 \pm 0.2) \times 10^{-10}$ for v=2, and $(4.1 \pm 0.3) \times 10^{-10}$ for $v = 4$ in units of cm^3 $molecule^{-1}$ s^{-1}. The errors denoted are 2σ. Time-dependent LIF intensities instead of absolute concentrations at left-hand side of eq 8 were used in the actual analysis. This does not lead to any error because LIF intensities are in proportion to the concentrations of the vibrational levels of interest.

Contrary to $v = 1$, 2, and 4, $v = 3$ shows a slightly positive curvature over a wide temporal range, because of the small difference between the decay rates of $v = 3$ and 4 (Figure 2b). The fact indicates that eq 8 for $v = 3$ cannot be approximated to be a single term even at large t and that the profiles must be represented by the following double-exponential form:

$$[OH(v=3)] = C_3 \exp(-k_3^{decay}t) + C_4 \exp(-k_4^{decay}t) \quad (9)$$

Because the decay of $v = 4$ is faster than that of $v = 3$, $C_3 > 0$ and $C_4 < 0$. In general, both decay rate constants k_3^{decay} and k_4^{decay} are adjusted to reproduce observed profiles. In the present case, because k_4^{decay} at different NH_3 pressures have already been obtained in the analysis of $v = 4$, only k_3^{decay} should be adjusted. This type of double-exponential fits is relatively easy, and k_3^{decay} is readily obtained. Observed profiles of LIF intensity were used also in this type of analysis. The NH_3 pressure dependence of apparent first-order decay rates gave k_3^{tot} to be $[3.3 \pm 0.4(2\sigma)] \times 10^{-10}$ cm^3 $molecule^{-1}$ s^{-1}.

We also analyzed the profiles of $v = 3$ by single-exponential fits. Resultant rate constants were dependent on the range of analysis and smaller than those obtained by the double-exponential fits. When a wide temporal range was analyzed (2−20 μs), k_3^{tot} was obtained to be 2.7×10^{-10} cm^3 $molecule^{-1}$ s^{-1}, and another analysis over 10−20 μs gave 3.0×10^{-10} cm^3 $molecule^{-1}$ s^{-1}. It is apparent that semilogarithmic analysis underestimates k_3^{tot}.

In order to confirm the validity of the double-exponential fits, we also adopted a linear integration analysis.[38,39] Because LIF intensities instead of concentrations of vibrational levels were recorded in experiments, and because the detectivities for vibrational levels are different and signal intensities are proportional to the absolute concentrations, the following equation is satisfied:

$$I_v(t) = \alpha_v[OH(v)] \quad (10)$$

where $I_v(t)$ and α_v are the observed LIF intensity at time t and detectivity for a vibrational level v, respectively. After the absolute concentration at time t, [OH(v=3)], in eq 7 is replaced with eq 10, the following expression is obtained: The integration

$$\frac{dI_3(t)}{dt} = k_{43}[NH_3]\frac{\alpha_3}{\alpha_4}I_4(t) - (k_3^{tot}[NH_3] + k_d)I_3(t) \quad (11)$$

of eq 11 from t_0 to t results in the following regression equation:

$$I_3(t) = I_3(t_0) + k_{43}[NH_3]\left(\frac{\alpha_3}{\alpha_4}\right)\int_{t_0}^{t} I_4(t)\,dt - (k_3^{tot}[NH_3] + k_d)\int_{t_0}^{t} I_3(t)\,dt \quad (12)$$

The integrated values to time t can be readily calculated, by a trapezoidal formula, from the time-dependent LIF signal intensities, $I_3(t)$ and $I_4(t)$, recorded in experiments. The lower limit of integration t_0 is set to the time after which a scheme composed of (4) and (6) are valid. In other words, t_0 must be positioned after the termination of the reaction $O(^1D) + NH_3 \rightarrow OH(v) + NH_2$ and the rotational relaxation of the nascent $OH(v)$. In the actual analysis, regression calculations were performed for more than 100 combinations of t_0 and t, and the regression coefficients obtained were averaged over all the combinations.

Multiple linear regression analysis using eq 12 gives $k_3^{tot}[NH_3] + k_d$ as a partial regression coefficient. Although another coefficient, $k_{43}[NH_3](\alpha_3/\alpha_4)$, is simultaneously obtained in the analysis, k_{43} and α_3/α_4 are not determined separately, and thus the branching ratios between relaxation and reactive removal are not derived. It, however, should be noted that total removal rate constant k_3^{tot} ($=k_{3,2} + k_3$) can be determined without the value of relative detectivity α_3/α_4. The fact indicates that the absolute concentrations of the vibrational levels are not needed. The values $k_3^{tot}[NH_3] + k_d$ measured at several NH_3 concentrations are plotted in Figure 3 along with the plot for $v = 4$, and the slope gives a collisional removal rate constant k_3^{tot} of $[3.5 \pm 0.4(2\sigma)] \times 10^{-10}$ cm^3 molecule^{-1} s^{-1}. This value is in excellent agreement with that obtained by the double-exponential fits. The small *negative* intercept of the plot of $v = 3$ has no physical meaning, because the 2σ error of the intercept is much larger, $\pm 2 \times 10^4$ s^{-1}, indicating that the rate of diffusion loss is negligible in the time scale observed. We have averaged the values of k_3^{tot} determined by the double-exponential fits and the linear integration analysis, and obtained deactivation rate constant for $v = 3$ by NH_3 as $[3.4 \pm 0.4(2\sigma)] \times 10^{-10}$ cm^3 molecule^{-1} s^{-1}.

An assumption was made that vibrational relaxation is limited to a single quantum change in the reaction scheme (4a). It is possible that multiquantum relaxation $\Delta v \geq 2$ occurs in collisions with NH_3. We also analyzed the same data with different schemes including relaxation $\Delta v \geq 2$; however, no significant rate constants for multiquantum relaxation ($\Delta v \geq 2$) were obtained. However, a decisive conclusion cannot be derived, because temporal overlap between two levels v and $v - 2$ are very small, and the data points are scarce. Observation of three consecutive levels with higher time resolution than the present study is necessary to evaluate the importance of relaxation with $\Delta v \geq 2$. An ideal way to judge the contribution of multiquantum relaxation is single level excitation to v_{ini} and observation of the time evolutions of the levels $v \leq v_{ini}$.

The overall rate constants k_v^{tot} for $OH(1 \leq v \leq 4) + NH_3$ are listed in Table 1 together with previously reported values. There have been several studies of the deactivation of $OH(v=1,2)$ by NH_3.[8,13,15−17,22] The reported values for $v = 1$ are somewhat scattered, but the differences are not so serious. Our rate constant for $v = 1$ is in excellent agreement with that recently reported by Silvente et al. The rate constant for $v = 2$ obtained in the present study agrees well with all the reported rate constants for $v = 2$.

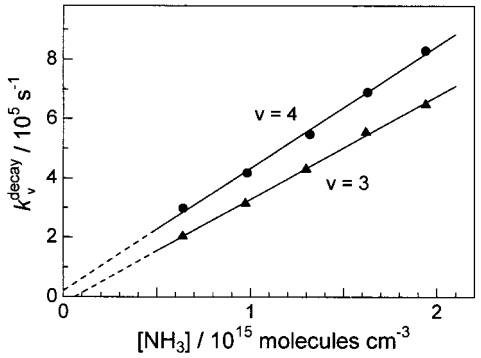

Figure 3. Pseudo-first-order decay rates k_v^{decay} for $OH(v=3,4)$ at various NH_3 pressures: solid circles, $v = 4$; solid triangles, $v = 3$.

There is only one report on deactivation rate constant for $OH(v=3)$ by NH_3. Cheskis et al.[13] have performed almost the same type of experiments as the present study. Their value, $(3.0 \pm 1.0) \times 10^{-10}$ cm^3 molecule^{-1} s^{-1}, is a little smaller than that obtained in the present study. It must, however, be added that the two values agree by virtue of the large confidence limits. Because Cheskis et al. did not show their profiles of $v = 3$, it is difficult to make clear the reason for the difference. Their large error might be due to the smallness of data points (at most 30 points), although this is by no means certain.

The rate constant for $v = 4$ obtained by the present study, is the first of the deactivation of $OH(v=4)$ by NH_3. The rate constant for $v = 4$ is only 17% larger than that for $v = 3$. As shown in Figure 4, the ratios of rate constants between adjacent vibrational levels decrease with vibrational quantum numbers: 3.8, 3.2, and 1.2 for $v = 2/v = 1$, $v = 3/v = 2$, and $v = 4/v = 3$, respectively. Unfortunately, there is no information on the branching ratios between vibrational relaxation and reactive removal on each vibrational level. Accordingly, vibrational energy dependence of *pure* vibrational relaxation rates cannot be discussed. If vibrational relaxation (4a) is predominant over reactive removal (4b), the large rate constants on the order of 10^{-11}−10^{-10} cm^3 molecule^{-1} s^{-1} might be due to the V−V energy transfer from $OH(v)$ to NH_3. The energy differences between adjacent levels of OH are 3570, 3404, 3240, and 3078 cm^{-1} for $v = 0$ and 1, $v = 1$ and 2, $v = 2$ and 3, and $v = 3$ and 4, respectively.[30] There are four vibrational modes of NH_3: 3337 cm^{-1} (ν_1), 950 cm^{-1} (ν_2), 3444 cm^{-1} (ν_3), 1627 cm^{-1} (ν_4); of these, ν_3 and ν_4 are doubly degenerate vibrations.[40] The ν_1 or ν_3 modes are the most preferable vibrational modes for accepting OH vibrational energies. The energy defects ΔE of the V−V vibrational energy transfer

$$OH(v) + NH_3 \rightarrow OH(v-1) + NH_3 + \Delta E \quad (13)$$

are +233, +67, −97, and −259 cm^{-1} for $v = 1$−4 and NH_3-(ν_1), and +126, −40, −204, and −366 cm^{-1} for $v = 1$−4 and $NH_3(\nu_3)$. When the mean translational energy at temperature T, $(3/2)RT = 311$ cm^{-1} at 298 K, is added to the defects, this results in the following *effective* defects: +544, +378, +214, and +52 cm^{-1} by $NH_3(\nu_1)$, and +437, +271, +107, and −55 cm^{-1} by $NH_3(\nu_3)$. The exponential energy gap model is given by the following equation:[41−43]

$$k_{V-V} = C \exp(-\beta|\Delta E|) \quad (14)$$

Because the present V−V energy transfers are governed by a dipole−dipole interaction, energy transfer probability is intrinsically proportional to the vibrational quantum number v.[43] Therefore, the quotient k_{V-V}/v instead of k_{V-V} should be used

TABLE 1: Total Removal Rate Constants for OH(v) + NH_3[a]

$v = 4$	$v = 3$	$v = 2$	$v = 1$	refs
		$(8 \pm 2.7) \times 10^{-11}$[b]	$(2.5 \pm 0.6) \times 10^{-11}$[b]	8
	$(3.0 \pm 1.0) \times 10^{-10}$	$(1.0 \pm 0.3) \times 10^{-10}$	$(2.1 \pm 0.3) \times 10^{-11}$	13
		$(1.2 \pm 0.15) \times 10^{-10}$		15, 16
		$(1.01 \pm 0.09) \times 10^{-10}$	$(2.49 \pm 0.21) \times 10^{-11}$	17
		$(1.26 \pm 0.12) \times 10^{-10}$	$(2.86 \pm 0.12) \times 10^{-11}$	22
$(4.1 \pm 0.3) \times 10^{-10}$	$(3.4 \pm 0.4) \times 10^{-10}$	$(1.1 \pm 0.2) \times 10^{-10}$	$(2.9 \pm 0.2) \times 10^{-11}$	this work[c]

[a] In units of cm^3 $molecule^{-1}$ s^{-1}. [b]Values were corrected using a more reliable rate constant for the reference reaction. [c]Errors denoted are 2σ.

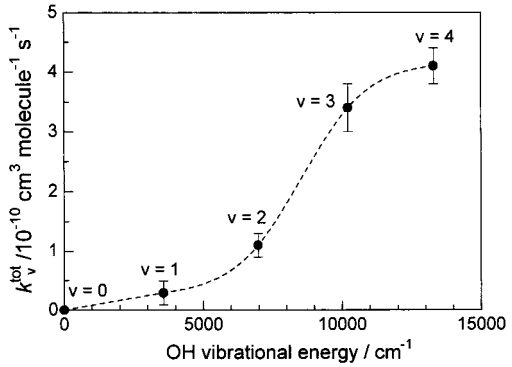

Figure 4. Vibrational energy dependence of total removal rate constants for $v = 0-4$. The error estimates shown are two standard deviations (2σ). Rate constants for $v = 1-4$ determined in the present study and reported value for $v = 0$[45] are plotted.

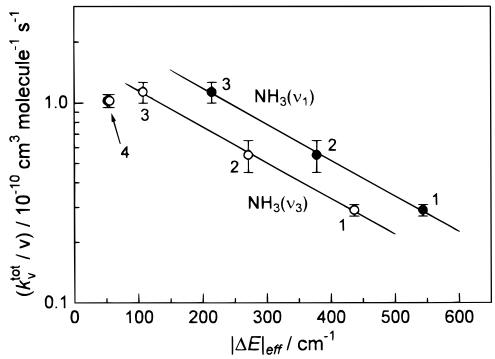

Figure 5. Normalized deactivation rate constants k_v^{tot}/v vs effective energy defect $|\Delta E|_{eff} = |\Delta E| + (3/2)RT$, where $|\Delta E|$ is defined by eq 13 in the text. Vibrational modes of NH_3 accepting OH vibrational energy are ν_1 (closed circles) and ν_3 (open circles). Vibrational quantum numbers of OH are written near the circles.

in eq 14.[17] Figure 5 shows the relation between the *normalized* rate constants and energy defects. The plots for $v = 1-3$ are nicely fitted by straight lines for both cases of energy acceptors ν_1 and ν_3. The regression lines give the parameter $\beta = 0.0041$ $(cm^{-1})^{-1}$. These findings suggest that the deactivation of OH(v=1−3) by NH_3 is mainly governed by the V−V energy transfer.

The rate constant for $v = 4$ deviates from the fit for the V−V energy transfer. This might indicate, not that $v = 4$ is deactivated by a different mechanism from $v \leq 3$, but that the overall rate constant reaches its ceiling (i.e., the gas-kinetic rate) at $v = 4$. Deactivation cross sections for $v = 1-4$ are 2.9, 13, 41, and 48 $Å^2$, respectively.

4. Conclusions and Future Directions

The overall deactivation rate constants of OH($X^2\Pi_i$, $v = 1-4$) by NH_3 have been determined. We have found that the rate constant for $v = 4$ is larger than that for $v = 3$ by only 17%, while $v = 3$ is 3.2 times as fast as $v = 2$ and $v = 2$ is 3.8 times faster than $v = 1$. The relatively small difference between the rate constants for $v = 3$ and 4 is due to the asymptotic approach to the gas-kinetic rate (Figure 4). Deactivation rates for $v = 1-3$ can be accounted for by the nonresonant V−V energy transfer from OH(v) to the ν_1 or ν_3 vibrational mode of NH_3, under the assumption that vibrational relaxation is predominant over reactive removal at every vibrational level (Figure 5). There has, however, been no report of direct evidence to prove the validity of this assumption. Because a the barrier for the chemical reaction OH + NH_3 → NH_2 + H_2O is about 7.7 kJ mol^{-1} over the temperature range 230−450 K,[44] even the lowest vibrationally excited level $v = 1$, with 43 kJ mol^{-1} of vibrational energy, might readily surmount the barrier. It is possible that the contribution of reactive removal to the overall deactivation increases with vibrational energies.

Branching ratios between vibrational relaxation and reactive removal could be determined if the relative detectivities α_{v-1}/α_v were known. The vibrational relaxation rate constant $k_{v,v-1}$ is obtained using α_{v-1}/α_v and NH_3 pressure dependence of the apparent first-order decay rate k_v^{decay} gives k_v^{tot} (= $k_{v,v-1}$ + k_v), and then k_v is derived from the overall rate constant. If the nascent vibrational distributions of OH produced in the O(^{1}D) + NH_3 reaction were known, $\alpha_v/\alpha_{v,v-1}$ could be determined.[24] Cheskis et al.[13] have determined the nascent vibrational distributions of OH in the O(^{1}D) + NH_3 reaction. They, however, have analyzed their data on the assumption that no reactive removal is present; therefore, their results cannot be used to determine the branching ratios between vibrational relaxation and reactive removal. Thus, information on the nascent vibrational distributions of OH is a key to extending the knowledge about the kinetics of vibrationally excited OH.

Acknowledgment. This work was supported by the Grant-in-Aid for Scientific Research on Priority Areas "Free Radical Science" (Contract No. 05237106) and Grant-in-Aids for Scientific Research (B) (Contract No. 08454181) and Grant-in-Aid for Scientific Research (C) (Contract No. 10640486) of the Ministry of Education, Science, Sports, and Culture.

References and Notes

(1) Meriwether, J. W. *J. Geophys. Res.* **1989**, *94*, 14629.
(2) Lyon, R. K. U.S. Patent 3,900, 554; August 1975.
(3) Lyon, R. K. *Int. J. Chem. Kinet.* **1976**, *8*, 315.
(4) DeMore, W. B.; Sander, S. P.; Golden, D. M.; Hampson, R. F.; Kurylo, M. J.; Howard, C. J.; Ravishankara, A. R.; Kolb, C. E.; Molina, M. J. *Chemical Kinetics and Photochemical Data for Use in Stratospheric Modeling*; JPL Publication 97-4; Jet Propulsion Laboratory, California Institute of Technology: Pasadena, CA, 1997.
(5) Spencer, J. E.; Glass, G. P. *Int. J. Chem. Kinet.* **1977**, *9*, 111.
(6) Spencer, J. E.; Glass, G. P. *Int. J. Chem. Kinet.* **1977**, *11*, 97.
(7) Greenblatt, G. D.; Wiesenfeld, J. R. *J. Geophys. Res.* **1982**, *87*, 11145.
(8) Glass, G. P.; Endo, H.; Chaturvedi, B. K. *J. Chem. Phys.* **1982**, *77*, 5450.
(9) Cannon, B. D.; Robertshaw, J. S.; Smith, I. W. M.; Williams, M. D. *Chem. Phys. Lett.* **1984**, *105*, 380.

(10) Smith, I. W. M.; Williams, M. D. *J. Chem. Soc., Faraday Trans. 2* **1985**, *81*, 1849.
(11) Smith, I. W. M.; Williams, M. D. *J. Chem. Soc., Faraday Trans. 2* **1986**, *82*, 1043.
(12) Brunning, J.; Derbyshire, D. W.; Smith, I. W. M.; Williams, M. D. *J. Chem. Soc., Faraday Trans. 2* **1988**, *84*, 105.
(13) Cheskis, S. G.; Iogansen, A. A.; Kulakov, P. V.; Sarkisov, O. M.; Titov, A. A. *Chem. Phys. Lett.* **1988**, *143*, 348.
(14) Teitelbaum, H.; Aker, P.; Sloan, J. J. *Chem. Phes.* **1988**, *119*, 79.
(15) Rensberger, K. J.; Jeffries, J. B.; Crosley, D. R. *J. Chem. Phys.* **1989**, *90*, 2174.
(16) Crosley, D. R.; Rensberger, K. J.; Jeffries, J. B. *AIP Conf. Proc.* **1989**, *191*, 615.
(17) Raiche, G. A.; Jeffries, J. B.; Rensberger, K. J.; Crosley, D. R. *J. Chem. Phys.* **1990**, *92*, 7258.
(18) Sappey, A. D.; Copeland, R. A. *J. Chem. Phys.* **1990**, *93*, 5741.
(19) Dodd, J. A.; Lipson, S. J.; Blumberg, W. A. M. *J. Chem. Phys.* **1991**, *95*, 5752.
(20) Chalamala, B. R.; Copeland, R. A. *J. Chem. Phys.* **1993**, *99*, 5807.
(21) Knutsen, K.; Dyer, M. J.; Copeland, R. A. *J. Chem. Phys.* **1996**, *104*, 5798.
(22) Silvente, E.; Richter, R. C.; Hynes, A. J. *J. Chem. Soc., Faraday Trans.* **1997**, *93*, 2821.
(23) Dyer, M. J.; Knutsen, K.; Copeland, R. A. *J. Chem. Phys.* **1997**, *107*, 7809.
(24) Yamasaki, K.; Watanabe, A.; Kakuda, T.; Ichikawa, N.; Tokue, I. *J. Phys. Chem.* **1999**, *103*, 451.
(25) Sappey, A. D.; Crosley, D. R.; Copeland, R. A. *J. Chem. Phys.* **1989**, *90*, 3484.
(26) Cleveland, C. B.; Jursich, G. M.; Trolier, M.; Wiesenfeld, R. *J. Chem. Phys.* **1987**, *86*, 3253.
(27) Park, C. R.; Wiesenfeld, J. R. *J. Chem. Phys.* **1991**, *95*, 8166.
(28) Yamasaki, K.; Tanaka, A.; Watanabe, A.; Yokoyama, K.; Tokue, I. *J. Phys. Chem.* **1995**, *99*, 15086.
(29) Baulch, D. L.; Cobos, C. J.; Cox, R. A.; Esser, C.; Frank, P.; Just, Th.; Kerr, J. A.; Pilling, M. J.; Troe, J.; Walker, R. W.; Warnatz, J. *J. Phys. Chem. Ref. Data* **1992**, *21*, 411.
(30) Huber, K. P.; Herzberg, G. *Molecular Spectra and Molecular Structure, IV. Constants of Diatomic Molecules*; Van Nostrand Reinhold: New York, 1979.
(31) Heard, D. E.; Crosley, D. R.; Jeffries, J. B.; Smith, G. P.; Hirano, A. *J. Chem. Phys.* **1992**, *96*, 4366.
(32) Kliner, D. A. V.; Farrow, R. L. *J. Chem. Phys.* **1999**, *110*, 412.
(33) McDade, I. C.; Llewellyn, E. J. *J. Geophys. Res.* **1987**, *92*, 7643.
(34) McDade, I. C. *Planet. Space Sci.* **1991**, *39*, 1049.
(35) Langhoff, S. R.; Werner, H.-J.; Rosmus, P. *J. Mol. Spectrosc.* **1986**, *118*, 507.
(36) Benson, S. W. *The Foundations of Chemical Kinetics*; Robert E. Krieger: Malabar, CA, 1982; pp 39−42.
(37) Holbrook, K. A.; Pilling, M. J.; Robertson, S. H. *Unimolecular Reactions*, 2nd ed.; John Wiley and Sons: Chichester, UK, 1996; Appendix 6.
(38) Yamasaki, K.; Watanabe, A. *Bull. Chem. Soc. Jpn.* **1997**, *70*, 89.
(39) Yamasaki, K.; Watanabe, A.; Kakuda, T.; Tokue, I. *Int. J. Chem. Kinet.* **1998**, *30*, 47.
(40) Herzberg, G. *Molecular Spectra and Molecular Structure, III. Electronic Spectra and Electronic Structure of Polyatomic Molecules*; Van Nostrand Reinhold: New York, 1966.
(41) Levine, R. D.; Bernstein, R. B. *Molecular Reaction Dynamics and Chemical Reactivity*; Oxford University Press: New York, 1987; Chapter 6.
(42) Polanyi, J. C.; Woodall, K. B. *J. Chem. Phys.* **1972**, *56*, 1563.
(43) Yardley, J. T. *Intramolecular Energy Transfer*; Academic Press: New York, 1980.
(44) Atkinson, R.; Baulch, D. L.; Hampson, R. F., Jr.; Kerr, J. A.; Troe, J. *J. Phys. Chem. Ref. Data* **1992**, *21*, 1125.
(45) Spencer, J. E.; Endo, H.; Grass, G. P. *Proc. 16th Symp. Combust.* **1976**.